ARTICLES
PUBLISHED ONLINE: 20 JANUARY 2013 | DOI: 10.1038/NCHEM.1550
nature chemistry

Molecular shape sorting using molecular organic cages

Tamoghna Mitra, Kim E. Jelfs, Marc Schmidtmann, Adham Ahmed, Samantha Y. Chong, Dave J. Adams and Andrew I. Cooper*

The energy-efficient separation of chemical feedstocks is a major sustainability challenge. Porous extended frameworks such as zeolites or metal–organic frameworks are one potential solution to this problem. Here, we show that organic molecules, rather than frameworks, can separate other organic molecules by size and shape. A molecular organic cage is shown to separate a common aromatic feedstock (mesitylene) from its structural isomer (4-ethyltoluene) with an unprecedented perfect specificity for the latter. This specificity stems from the structure of the intrinsically porous cage molecule, which is itself synthesized from a derivative of mesitylene. In other words, crystalline organic molecules are used to separate other organic molecules. The specificity is defined by the cage structure alone, so this solid-state 'shape sorting' is, uniquely, mirrored for cage molecules in solution. The behaviour can be understood from a combination of atomistic simulations for individual cage molecules and solid-state molecular dynamics simulations.

The separation of molecules by fractional distillation is a key process in industry, but it can also involve large energy costs. Chemists have therefore developed a range of synthetic porous solids for the more energy-efficient separation of commercially important chemicals such as alkanes and alkenes[1], structural[2,3] and geometric[4,5] hydrocarbon isomers, and chiral molecules[6,7]. Most studies have focused on extended porous frameworks such as inorganic zeolites[8] or hybrid metal–organic frameworks (MOFs)[9], which are useful in separation technologies such as chromatography. Certain organic molecules can also distinguish between closely related chemical species in solution, but not in the solid state. The best-known examples are crown ethers, which bind some metal ions selectively[10], but a wide range of other macrocycles[11], molecular cages[12] and capsules[13] can also exhibit solution-phase guest selectivity. In principle, well-defined molecular selectivity or specificity in solution could translate into the solid state, provided that the host molecules can assemble into a solid, porous form (Fig. 1); in other words, organic molecules might be designed to separate other organic molecules. Until now, however, the host–guest behaviour of molecules in solution and in related crystalline solids has only been considered separately.

Here, we examine the guest selectivity of intrinsically porous organic cage molecules[14]. These cage compounds can be synthesized from C_3 trialdehydes and 1,2-substituted vicinal diamines by a simple condensation reaction (Fig. 2). The shape of the cavity in these cages and in particular the geometry of their *meta*-substituted aryl faces suggests their potential for size- and shape-selective guest binding (Fig. 3a). We focused initially on C8 and C9 aromatic molecules such as xylenes and mesitylene and its isomers, which are important chemical feedstocks. These aromatic molecules, unlike alkenes and alkanes[1], do not lend themselves to separation by open-metal coordination sites, a process that exploits the presence or absence of double bonds in the molecules to be separated. Hence, separation by molecular shape is more viable for C8 and C9 aromatic isomers and other molecules that differ mainly in their shape.

Results

We studied the selectivity of these cage molecules in four different ways. First, we used molecular simulations for individual cages in the gas phase to evaluate the shape match between host and guest, and also the flexibility of the cage host. Second, we carried out solution-phase binding studies to examine host–guest binding interactions for discrete organic cages in solution. Third, we performed sorption experiments using cages in the solid, crystalline state, and evaluated these organic cages as solid-phase chromatography media. Finally, we carried out molecular dynamics (MD) simulations for the crystalline organic materials to rationalize diffusion mechanisms in the solid state. Our aim was to establish whether the structure of the molecular cage, taken in isolation, can be used to predict solid-state sorption behaviour, thus allowing

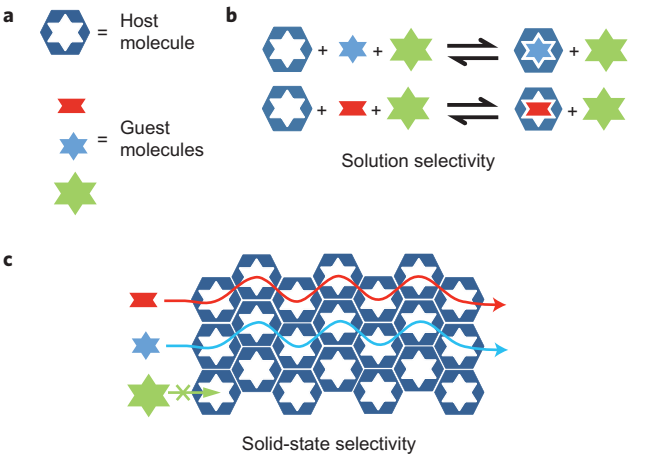

Figure 1 | Molecules to separate molecules. a–c, A discrete host molecule (**a**) has shape and size selectivity for guest molecules in solution (**b**), which can translate into the solid state providing that the host molecule assembles to form a porous solid (**c**).

Department of Chemistry and Centre for Materials Discovery, University of Liverpool, Brownlow Hill, Liverpool, Merseyside L69 3BX, UK.
*e-mail: aicooper@liverpool.ac.uk

© 2013 Macmillan Publishers Limited. All rights reserved.

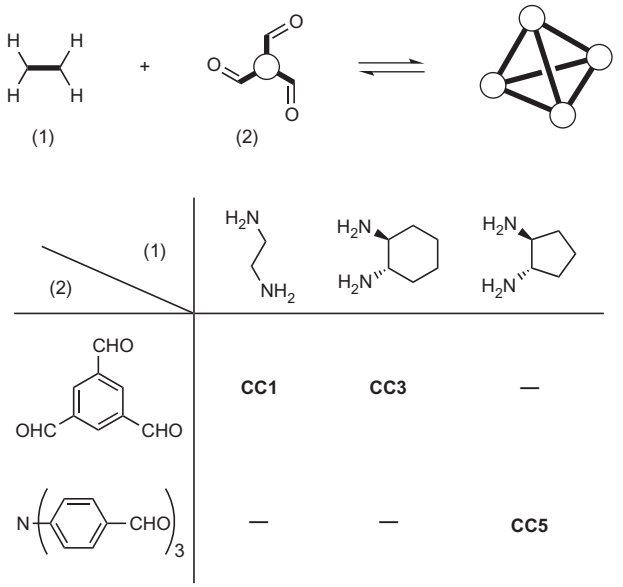

Figure 2 | Synthesis of organic cages. General scheme for preparing [4 + 6] organic cages via a cycloimine condensation reaction.

strategies where bespoke cage molecules are tailored to specific molecular separations.

Gas-phase molecular simulations for single cages. We first studied the host–guest behaviour of isolated organic cages in the gas phase to evaluate the influence of the discrete molecular cage in the absence of any crystal packing forces. Molecular models for two structurally related cages, CC1 (which has ethane vertices; Fig. 3b, left) and CC3 (which has cyclohexane vertices; Fig. 3b, right), both indicate a close geometric fit inside the cage cavity for a C9 guest, mesitylene. For these cages, one of the building units[14] (1,3,5-triformylbenzene) is isostructural with the guest, mesitylene. Indeed, mesitylene is a precursor for 1,3,5-triformylbenzene. Hence, by choosing appropriate cage building units, the host structure can be made to mimic the structure of a particular guest. Although CC1 and CC3 are geometrically similar, the two cages have quite different molecular rigidity. Gas-phase MD simulations were carried out for cages containing a single mesitylene guest. The mesitylene molecule was observed to turn or 'flip' within the CC1 cage a total of eight times during a 2 ns simulation. In contrast, mesitylene does not flip in the more rigid CC3 cage over the same timescale, remaining π-stacked with one face of the cage. These simulations suggest that CC1 and CC3 might have quite different solution and solid-state host–guest chemistry for mesitylene.

Solution-phase host–guest binding measurements. To test the findings of these gas-phase simulations for discrete cage molecules, we carried out corresponding solution-phase studies, exploiting the fact that the cage building units are soluble in common organic solvents. We first prepared both guest-loaded CC1 and CC3 by synthesizing the two cages in the presence of excess mesitylene. The products were characterized by single-crystal X-ray diffraction. The resulting crystals, mesitylene@CC1 (ref. 15) and mesitylene@CC3 (Supplementary Fig. S1), both have a single mesitylene molecule encapsulated inside each cage. When the mesitylene@CC3 crystals were dissolved in a solvent ($CDCl_3$), NMR measurements confirmed entrapment of the mesitylene

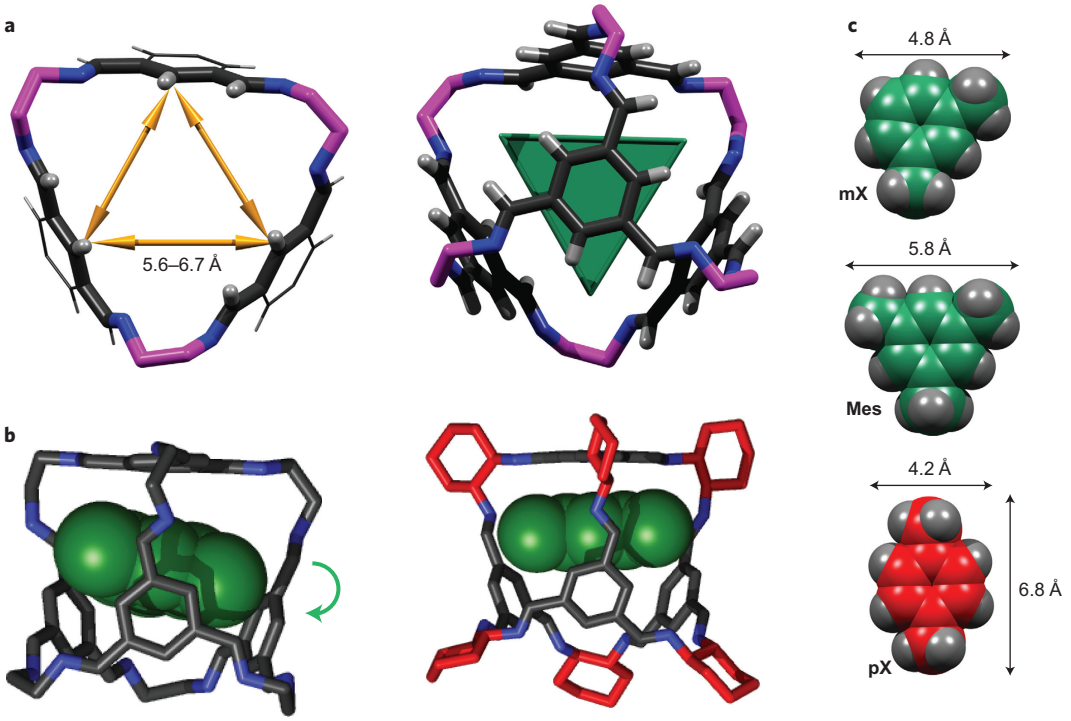

Figure 3 | Solid-state shape selectivity can be understood in terms of the structure and dynamics of discrete, isolated cage molecules. a, Left: framework structure for porous cages CC1 and CC3, highlighting the triangular cage window that is described by three aromatic hydrogen atoms (range of interatomic distances indicated by yellow double-headed arrows). The 1,2-bisimine cage vertices (coloured pink) are ethane for cage CC1 and cyclohexane for cage CC3. Each tetrahedral cage molecule has four approximately triangular windows. Right: the 1,3,5-substituted aromatic cage building block generates a cavity with a three-fold axis of symmetry, as illustrated by the green triangle. Both *meta*-xylene (**mX**) and mesitylene (Mes) have 1,3-substituted geometries that match this cavity geometry, whereas *para*-xylene (pX) does not. **b**, Gas-phase MD simulations at 273 K for isolated cage molecules show that the mesitylene guest (green) can turn inside the cavity of CC1 (left), but does not turn in the same time period for the more rigid cage, CC3 (right). Hydrogens are omitted for clarity in **b**. **c**, Relative dimensions of the guests mX, Mes and pX.

© 2013 Macmillan Publishers Limited. All rights reserved.

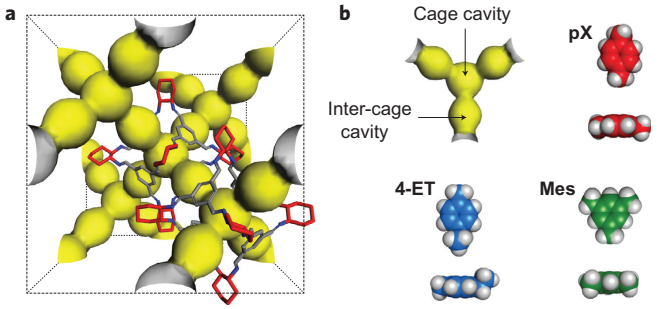

Figure 4 | The diamondoid pore network for crystalline CC3 carries the steric signature of the discrete cage building units. a, Connolly surface for **CC3** calculated with a probe radius of 2.5 Å. Two cages are illustrated, demonstrating the window-to-window crystal packing. **b**, Shape comparison of a single node in the pore network (with the fourth channel going into the page), illustrated on the same scale as the guests *para*-xylene (**pX**), 4-ethyltoluene (**4-ET**) and mesitylene (**Mes**), as viewed perpendicular to both the aryl plane (upper) and the long axes of these molecules (lower).

guest within the cage (Supplementary Fig. S2). We observed a slow release of the mesitylene guest from mesitylene@**CC3** in solution, with a half-life of ~2.5 days (Supplementary Fig. S4). This slow release process could be greatly accelerated by the addition of a catalytic amount trifluoroacetic acid, suggesting that release of the guest occurs by reversible breaking of the dynamic imine bonds in **CC3** (refs 15,16). In contrast, when mesitylene@**CC1** crystals were dissolved in $CDCl_3$, the trapped mesitylene guest was displaced immediately by the solvent, and only free mesitylene was observed by ^{1}H NMR spectroscopy. This indicates that the more flexible **CC1** molecule allows the guest to escape in solution, in line with the greater flexibility observed for this cage in gas-phase MD simulations.

An analogous synthesis of **CC3** in the presence of a smaller guest, *meta*-xylene, produced the isostructural compound *meta*-xylene@**CC3**, as characterized by single-crystal X-ray diffraction (Supplementary Fig. S6). However, unlike mesitylene@**CC3** (2.5 day half-life in $CDCl_3$), *meta*-xylene@**CC3** released its guest in $CDCl_3$ solution immediately upon dissolution. Hence, *meta*-xylene (Fig. 3a) is small enough to pass through the cage window, even in the relatively inflexible **CC3** molecule.

Solid-state selectivity measurements. The results of both gas-phase MD simulations and solution-phase NMR experiments suggested that crystals of the more rigid cage, **CC3**, might have the potential to separate aromatic molecules such as *meta*-xylene, mesitylene and related species. We therefore studied the solid–vapour sorption properties of crystalline **CC3** for a range of C8 and C9 aromatics that are important chemical feedstocks. The empty **CC3** host crystallizes in a cubic form[14], with the four windows of each cage aligned with the window of a neighbouring cage, resulting in an extended diamondoid pore channel network (Fig. 4).

Because these pore channels run through the internal cavity and windows of the cages, the channel topology bears the 'steric signature' of the individual cage molecule. Hence, the gas-phase MD calculations and the host–guest behaviour in solution might be reasonable proxies for the solid-state sorption properties of **CC3**. This situation is very different from extended frameworks such as zeolites and metal–organic frameworks where the molecular building blocks, taken in isolation, give essentially no information about the sorption properties of the resulting three-dimensional self-assembled solids.

To test this concept, we carried out vapour adsorption studies for single-component C8 and C9 aromatics in solid **CC3**. The first observation was that mesitylene vapour was rejected completely by the **CC3** crystals (Fig. 5a), in line with the solution-phase NMR experiments. That is, without breaking imine bonds by hydrolysis—which we have shown not to occur in the solid state[17]—mesitylene cannot diffuse through the windows of **CC3**. In contrast, solid **CC3** does adsorb a C9 structural isomer of mesitylene—4-ethyltoluene—which has a different, more linear shape. The two isomers 4-ethyltoluene and mesitylene have similar molecular volumes (calculated as 140.2 Å^3 and 149.5 Å^3, respectively), and we ascribe this marked difference predominantly to the guest shape, rather than to size.

The exclusion of mesitylene in crystalline **CC3** occurs because the geometry and size of the cage host and guest are closely matched. For example, an expanded cage, **CC5** (ref. 18), is not close in size to these C9 guests, and although it forms an analogous diamondoid pore structure, it does not show significant selectivity between mesitylene and 4-ethyltoluene (Supplementary Tables S2 and S3). The steric exclusion of mesitylene in **CC3** was also demonstrated by a simple experiment where we submerged a **CC3** crystal, preloaded with physisorbed CO_2 gas, into pure mesitylene. Because mesitylene is too large to pass through the windows of **CC3**, it does not replace the physisorbed gas within the pores. However, when the structural isomer 4-ethyltoluene is added, CO_2 is displaced from the pores in **CC3**, as demonstrated by rapid gas evolution from the surface of the crystal (Supplementary Movie S1).

As well as distinguishing the shapes of the C9 structural isomers mesitylene and 4-ethyltoluene, **CC3** crystals also have different sorption characteristics for *para*-, *meta*- and *ortho*- positional isomers of C8 and C9 disubstituted aromatics. In general, *para* isomers are most preferred, followed by *meta* isomers, with *ortho* isomers being adsorbed more slowly, both for C9 (Fig. 5a) and C8 (Fig. 5b) aromatic molecules. To better understand the selectivity of solid **CC3** for these positional isomers, we characterized the crystals by single-crystal X-ray diffraction after loading with *para*-xylene and *meta*-xylene. In the *para*-xylene-loaded crystals, the xylene guest was found to occupy the inter-cage channel cavity, which connects two adjacent cage molecules (Fig. 5d), rather than the central cage cavity itself. In contrast, the *meta*-xylene isomer sits, like entrapped mesitylene, π-stacked in the cavity of each cage (Fig. 5c). The saturation uptake capacity of crystalline **CC3** for these C8 molecules is therefore defined by the shape of the guest: *meta*-xylene matches the shape of the cage cavity, which has a three-fold axis of symmetry (Fig. 3a), while the linear inter-cage cavities of the diamondoid channel can more easily accommodate *para*-xylene. This leads to a stoichiometric preference for *para*-xylene over *meta*-xylene of 2:1 (Fig. 5b) in these non-competitive sorption experiments because there are twice as many inter-cage cavities as cage cavities in the crystal.

Chromatographic separations. These kinetic sorption studies inspired us to test the dynamic separation of mesitylene from its positional isomer, 4-ethyltoluene, in a continuous-flow setup using a chromatography column packed with **CC3** crystals. This is possible because the **CC3** molecule, while soluble in halogenated solvents such as chloroform or dichloromethane, has extremely low solubility in aromatic solvents such as xylene or mesitylene. The breakthrough plot shows that mesitylene elutes as soon as it is pumped into the absorbent bed, while 4-ethyltoluene is retained by the cage sorbent (Fig. 5e,f). This illustrates that gas-phase MD simulations for isolated cage molecules can be used to anticipate real-life chromatographic performance, at least for systems that crystallize to produce pore windows and channels that are defined by the intrinsic molecular pores.

Solid-state molecular simulations. We were initially surprised that the *para*-xylene and 4-ethyltoluene molecules were able to diffuse into **CC3** in the solid state, because the diameters of these guests

© 2013 Macmillan Publishers Limited. All rights reserved.

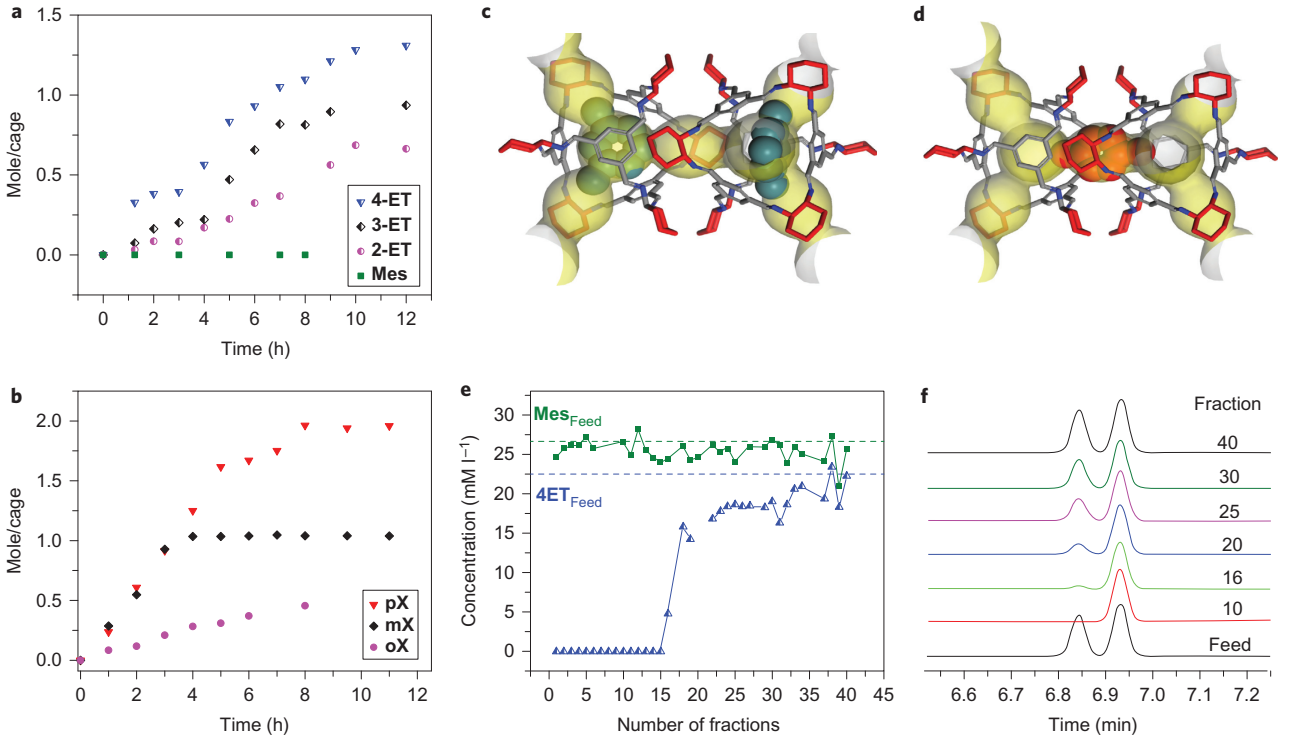

Figure 5 | Solid-state shape selectivity and chromatographic separations using crystalline porous organic cages. a, Time-dependent guest uptakes for C9 aromatic isomers (C_9H_{12}) in crystalline **CC3** (single-component measurements). **Mes**, mesitylene; **4-ET**, 4-ethyltoluene; **3-ET**, 3-ethyltoluene; **2-ET**, 2-ethyltoluene. The cage molecule totally excludes the mesitylene isomer. **b**, Equivalent guest uptakes for C8 aromatics (C_8H_{10}) *para*-xylene (**pX**), *meta*-xylene (**mX**) and *ortho*-xylene (**oX**). **c**, X-ray crystallography and sorption simulations reveal the preferred docking sites for the *meta*- and *para*-xylene isomers. *Meta*-xylene (green) fits in the centre of each cage. **d**, In contrast, *para*-xylene (orange) is accommodated in the linear inter-cage cavity. The 2:1 ratio of the saturation uptake capacities for **pX** and **mX** occurs because there are twice as many inter-cage cavities in the crystal. **e**, Breakthrough experiment for a mixture of the C9 structural isomers mesitylene and 4-ethyltoluene. **f**, Gas chromatograms for separated fractions. The peak on the left is 4-ethyltoluene.

are larger than the narrowest point in the pore channels, which is 5.32 Å at the cage window. Moreover, to diffuse through the **CC3** structure, these guests must pass through the windows of neighbouring cages and then undergo a 'flip' within the tetrahedral cage cavity to access a new window (Supplementary Fig. S11). From inspection of the static **CC3** crystal structure, it seemed intuitive that linear molecules such as *para*-xylene and 4-ethyltoluene might not be able to negotiate this tetrahedral intersection. The unanticipated sorption behaviour of *para*-xylene and 4-ethyltoluene (Fig. 5a,b) led us to explore the diffusion mechanism for these molecules using solid-state MD simulations[19].

Docking calculations confirmed the preferred experimental sorption locations for *para*-xylene, 4-ethyltoluene and mesitylene (Supplementary Fig. S12). Next, solid-state MD simulations were performed for these three species. Analysis of the simulated trajectories of the three sorbates in **CC3** showed that both *para*-xylene and 4-ethyltoluene diffused throughout the crystal, while the mesitylene molecule remained trapped in its starting cage, as shown in Fig. 6b (Supplementary Fig. S13 and Movies S2–S4). Repeating the *para*-xylene simulations with the cages held fixed as rigid bodies prevented the guest diffusing at all. This demonstrates that, even for the relatively rigid **CC3**, molecular flexibility is essential for guest diffusion[20], permitting the cage windows to breathe to allow passage of the guest. For example, analysis of a trajectory where the *para*-xylene is passing through a cage window shows that the window has breathed by more than 2 Å to a diameter of 7.40 Å, which is significantly larger than the diameter of *para*-xylene (5.8 Å). Flexibility also allows the cage voids to swell, thus providing sufficient space for the guests to turn within the cage.

Figure 6a demonstrates that 4-ethyltoluene takes longer than *para*-xylene to visit all 32 of the cages in the simulation cell, and that mesitylene does not diffuse at all on this timescale. The trend in the simulated diffusion kinetics for these three guests agrees qualitatively with the experimental measurements for solid crystalline **CC3** shown in Fig. 5a,b.

To negotiate the cage cavity and to leave by another window, these approximately linear sorbates must 'flip' within the cage by π-stacking to a different arene face. Calculation of the energy barriers for *para*-xylene diffusion in the solid state (Fig. 6c) shows that the diffusion pathway has three energetic barriers, two corresponding to the two widest parts of the *para*-xylene guest molecule passing through a window and a third corresponding to the guest turning within a cage. The energy profile suggests that the rate-determining step for *para*-xylene diffusion in **CC3** is 'flipping' within the cage cavity, rather than passage through the narrow cage windows, and the MD simulations show that this is only possible because of a degree of flexibility in this crystalline organic solid.

Discussion

Our results show that porous organic molecules can be used for the solid-state separation of other organic molecules. In the case of two C9 structural isomers, this occurs with total specificity. Uniquely, this can be correlated with host–guest behaviour for discrete cage molecules in solution. The one-pot cage syntheses themselves are quite scalable[21], and these results suggest that other organic cages could be designed to mimic the size and shape of particular guests, and hence to achieve specific separations. Larger porous organic cages have also been prepared that might be suitable for the separation of larger guests[22]. Conceivably, this approach could also be used to fabricate shape-selective, solid-state molecular sensors[20], exploiting the solution processability of the cages, or materials that selectively capture harmful organic pollutants.

© 2013 Macmillan Publishers Limited. All rights reserved.

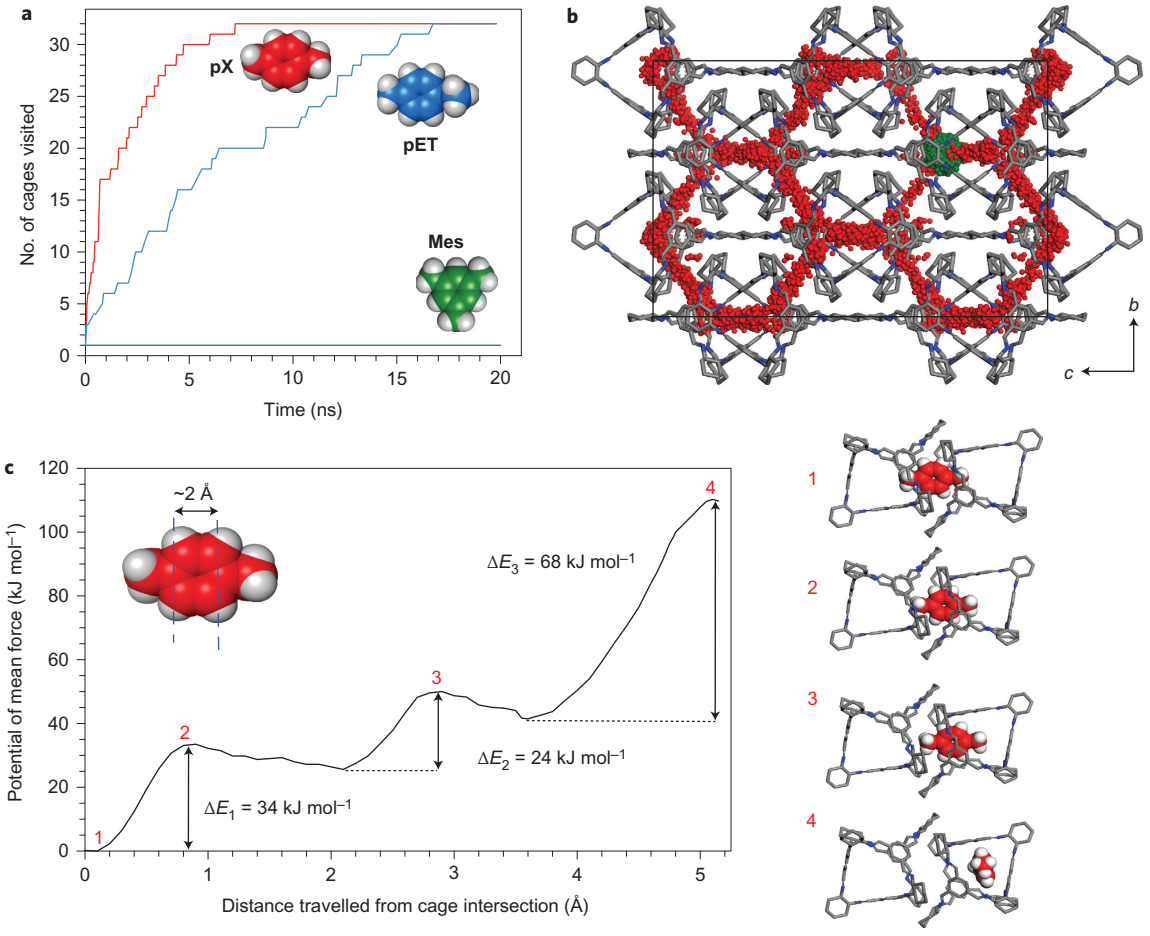

Figure 6 | Solid-state molecular simulations reveal diffusion mechanisms for the organic guests. a, Graph showing the cumulative number of cages visited over a 20 ns canonical ensemble (NVT) MD simulation at 750 K for three sorbates: *para*-xylene (**pX**), 4-ethyltoluene (**4-ET**) and mesitylene (**Mes**). There are a total of 32 cages in the 2 × 2 × 2 supercell. These results agree qualitatively with the measurements shown in Fig. 5a,b. **b**, The centre of mass of *para*-xylene (red) and mesitylene (green) positions sampled during the simulation are overlaid on the starting configuration for the guest-free *para*-xylene@**CC3** structure. **c**, Graph showing the potential of mean force as a function of the linear distance travelled by a *para*-xylene through the **CC3** host. The guest starts at an intersection between two cages (1), then moves into a cage by passing through one of its windows. Points (2) and (3) correspond to the two widest parts of the *para*-xylene molecule (marked with dashed blue lines in the inset) passing through the window to enter a new cage. At (4), the guest has rotated or 'flipped' within the cage, ready to exit from another window; this is the largest energy barrier to diffusion.

We believe that this strategy is complementary to recent advances in MOFs that involve separation via chemical differentiation by open metal centres[1]. Although the separation of structural and positional organic isomers has also been achieved in porous extended frameworks[2–5], this new molecular approach offers some potential advantages. For example, unlike all extended frameworks, these molecular organic cages are soluble in common organic solvents, so they are readily processed into well-defined nanoparticles[23], and can also be co-processed directly into composite films and membranes[24]. We therefore envisage strategies where shape-selective molecular organic pores are added from organic solution into more complex functional composites, recognizing that insoluble microcrystalline powders may be difficult to process and hence unsuitable for some applications. Porous organic cages such as **CC3** can also be homochiral, and there is potential to extend the approach to chiral separations, or possibly to tandem processes that involve separation by both shape and by chirality.

There are also some future challenges to consider. For example, molecular solubility, while useful for processing, would be highly undesirable in a liquid-phase chromatographic process. The solubility of **CC3** in liquids such as mesitylene and 4-ethyltoluene is extremely low, however, and we have also developed strategies for preparing porous racemates that are effectively insoluble in some cases[22]. Another challenge is sorption kinetics: ideally, high selectivity would be combined with high guest diffusion rates, but in practice it can be difficult to combine these two properties in a single solid. We are evaluating approaches to generate materials with hierarchical porosity, building on the fact that more than one organic cage can be co-crystallized into a single porous organic solid[18].

Methods

Materials. 1,3,5-Triformylbenzene was purchased from Manchester Organics. All other chemicals were purchased from Sigma-Aldrich and used as received, unless otherwise stated. **CC1**, **CC3** and **CC5** were prepared according to methods described previously[18].

Synthesis of mesitylene@CC3. (*R,R*)-1,2-Diaminocyclohexane (53 mg, 0.465 mmol) was dissolved in a mixture of mesitylene and dichloromethane (DCM, 30 ml, 2.5:1 vol/vol). The resulting solution was added dropwise to a stirred solution of 1,3,5-triformylbenzene (50 mg, 0.31 mmol in 10 ml DCM) over a period of 90 min. The resulting mixture was left covered for 3–4 weeks at 20–22 °C. White, needle-like crystals of the product were filtered off after 4 weeks. The crystals were washed with a DCM–mesitylene mixture (5:95 vol/vol), dried in air, and then finally dried under vacuum at ambient temperature (yield, ~85 mg). An analogous procedure was used to prepare *meta*-xylene@**CC3** (Supplementary Section S1.2).

Vapour-phase and liquid-phase adsorption experiments. In addition to solid-state sorption experiments for single-component C8 and C9 aromatics (Fig. 5a,b), competitive sorption experiments were also carried out with mixed C9 hydrocarbon isomers. For each vapour-phase experiment, an open 5 ml vial containing 0.020 g of

© 2013 Macmillan Publishers Limited. All rights reserved.

the guest-free CC3 adsorbent was placed in a sealed 40 ml vial containing 1 ml of a binary (equimolar) mixture of C9-alkylaromatics. Uptake in the CC3 crystals was measured after 24 h by completely dissolving the crystals and measuring the C9-alkylaromatic ratio by ^{1}H NMR. The relative uptakes of different guests are tabulated in Supplementary Tables S2 and S3. Methods for liquid-phase batch experiments are detailed in the Supplementary Section S2.1 and Fig. S9.

Liquid-phase breakthrough experiment. To obtain the data shown in Fig. 5e,f, breakthrough experiments were performed using a 5 cm stainless-steel column with an internal diameter of 4 mm. The column was packed with CC3 (230 mg) and silica gel (230 mg), the latter added to reduce the back pressure, and the packed column was attached to a syringe pump. For breakthrough analysis, each fraction (~0.15 ml) was collected directly at the column outlet. The concentrations of the different components in each fraction were analysed by gas chromatography.

Molecular simulations. Full details are given in the Supplementary Information. Docking calculations attempted to load a single guest molecule into the CC3 host structure using the Materials Studio Adsorption Locator module and an in-house cage-specific forcefield (CSFF)[25]. There were 100,000 initial insertion steps, followed by three cycles of 50,000 steps to anneal the docked location if the insertion was successful. MD simulations of sorbate mobility in single isolated cages were carried out using the DL_POLY2.20 program. A sorbate was placed in the void of a single cage in the centre of a (50 × 50 × 50) Å^3 empty cubic cell. The cells were equilibrated for 200 ps using the canonical (NVT) ensemble, with constant volume and temperature, with the Nosé–Hoover[26] thermostat at 273 K, the velocity verlet algorithm, a relaxation time of 0.5 ps, and a timestep of 0.5 fs. This was then followed by a 2 ns production run. The simulation was sampled every 0.05 ps. Solid-state MD simulations were also carried out in DL_POLY2.20 to investigate the mobility of the various sorbates in the bulk crystal structure. A (35.356 × 35.782 × 49.756) Å^3 supercell containing 32 CC3 cages was used, starting with the *para*-xylene@CC3 structure with the *para*-xylene guests deleted. A single molecule of each of the three sorbates was started in the most energetically favourable location found from the above docking calculations. The cells were equilibrated for 200 ps using the NPT (constant temperature and pressure) ensemble with the Nosé–Hoover thermostat and barostat at 750 K, the leapfrog verlet algorithm[27] to integrate Newton's equations of motion, a pressure of 1 atm, a relaxation time of 0.5 ps, and a timestep of 0.7 fs. The final configuration of this NPT ensemble simulation was then used to run a 20 ns NVT simulation at 750 K with the Nosé–Hoover thermostat to observe the guest mobility (timestep of 0.7 fs; system sampled every 1.75 ps). To investigate the influence of the cage flexibility upon the motion of these organic guests, a 20 ns NPT molecular dynamics simulation at 750 K was carried out with all the CC3 cages held fixed as rigid bodies using the QSHAKE algorithm to apply the rigid body constraints within DL_POLY2.20. No diffusion was observed in this case for any guests. Methods for the potential of mean force (PMF) free-energy calculations are described in the Supplementary Information.

Received 9 August 2012; accepted 7 December 2012; published online 20 January 2013

References

1. Bloch, E. D. *et al.* Hydrocarbon separations in a metal–organic framework with open iron(II) coordination sites. *Science* **335,** 1606–1610 (2012).
2. Alaerts, L. *et al.* Selective adsorption and separation of *ortho*-substituted alkylaromatics with the microporous aluminum terephthalate MIL-53. *J. Am. Chem. Soc.* **130,** 14170–14178 (2008).
3. Alaerts, L. *et al.* Selective adsorption and separation of xylene isomers and ethylbenzene with the microporous vanadium(IV) terephthalate MIL-47. *Angew. Chem. Int. Ed.* **46,** 4293–4297 (2007).
4. Alaerts, L., Maes, M., van der Veen, M. A., Jacobs, P. A. & De Vos, D. E. Metal–organic frameworks as high-potential adsorbents for liquid-phase separations of olefins, aklylnaphthalenes and dichlorobenzenes. *Phys. Chem. Chem. Phys.* **11,** 2903–2911 (2009).
5. Maes, M. *et al.* Separation of C_5-hydrocarbons on microporous materials: complementary performance of MOFs and zeolites. *J. Am. Chem. Soc.* **132,** 2284–2292 (2010).
6. Vaidhyanathan, R. *et al.* A family of nanoporous materials based on an amino acid backbone. *Angew. Chem. Int. Ed.* **45,** 6495–6499 (2006).
7. Nuzhdin, A. L., Dybtsev, D. N., Bryliakov, K. P., Talsi, E. P. & Fedin, V. P. Enantioselective chromatographic resolution and one-pot synthesis of enantiomerically pure sulfoxides over a homochiral Zn–organic framework. *J. Am. Chem. Soc.* **129,** 12958–12959 (2007).
8. Kulprathipanja, S. & James, R. B. in *Zeolites in Industrial Separation and Catalysis* (ed. Kulprathipanja, S.) 173–202 (Wiley-VCH, 2010).
9. Li, J-R., Sculley, J. & Zhou, H. C. Metal–organic frameworks for separations. *Chem. Rev.* **112,** 869–932 (2011).
10. Pedersen, C. J. The discovery of crown ethers. *Angew. Chem. Int. Ed. Engl.* **27,** 1021–1027 (1988).
11. Tashiro, S., Kubota, R. & Shionoya, M. Metal–macrocycle framework (MMF): supramolecular nano-channel surfaces with shape sorting capability. *J. Am. Chem. Soc.* **134,** 2461–2464 (2011).
12. Mastalerz, M. Shape-persistent organic cage compounds by dynamic covalent bond formation. *Angew. Chem. Int. Ed.* **49,** 5042–5053 (2010).
13. Dube, H. & Rebek, J. Selective guest exchange in encapsulation complexes using light of different wavelengths. *Angew. Chem. Int. Ed.* **51,** 3207–3210 (2012).
14. Tozawa, T. *et al.* Porous organic cages. *Nature Mater.* **8,** 973–978 (2009).
15. Hasell, T. *et al.* Triply interlocked covalent organic cages. *Nature Chem.* **2,** 750–755 (2010).
16. Ro, S., Rowan, S. J., Pease, A. R., Cram, D. J. & Stoddart, J. F. Dynamic hemicarcerands and hemicarceplexes *Org. Lett.* **2,** 2411–2414 (2000).
17. Hasell, T., Schmidtmann, M., Stone, C. A., Smith, M. W. & Cooper, A. I. Reversible water uptake by a stable imine-based porous organic cage. *Chem. Commun.* **48,** 4689–4691 (2012).
18. Jones, J. T. A. *et al.* Modular and predictable assembly of porous organic molecular crystals. *Nature* **474,** 367–371 (2011).
19. Smith, W., Yong, C. W. & Rodger, P. W. DL_POLY: application to molecular simulation. *Mol. Simul.* **28,** 385–471 (2002).
20. Brutschy, M., Schneider, M. W., Mastalerz, M. & Waldvogel, S. R. Porous organic cage compounds as highly potent affinity materials for sensing by quartz crystal microbalances. *Adv. Mater.* **24,** 6049–6052 (2012).
21. Lydon, D. P., Campbell, N. L., Adams, D. J. & Cooper, A. I. Scalable synthesis for porous organic cages. *Synth. Commun.* **41,** 2146–2151 (2011).
22. Mastalerz, M., Schneider, M. W., Oppel, I. M. & Presly, O. A salicylbisimine cage compound with high surface area and selective CO_2/CH_4 adsorption. *Angew. Chem. Int. Ed.* **50,** 1046–1051 (2010).
23. Hasell, T., Chong, S. Y., Jelfs, K. E., Adams, D. J. & Cooper, A. I. Porous organic cage nanocrystals by solution mixing. *J. Am. Chem. Soc.* **134,** 588–598 (2012).
24. Bushell, A. F. *et al.* Nanoporous organic polymer/cage composite membranes, *Angew. Chem. Int. Ed.* http://dx.doi.org/10.1002/anie.201206339 (2012).
25. Holden, D. *et al.* Bespoke force field for simulating the molecular dynamics of porous organic cages. *J. Phys. Chem. C* **116,** 16639–16651 (2012).
26. Hoover, W. G. Canonical dynamics – equilibrium phase-space distributions. *Phys. Rev. A* **31,** 1695–1697 (1985).
27. Forester, T. R. & Smith, W. SHAKE, rattle, and roll: efficient constraint algorithms for linked rigid bodies. *J. Comput. Chem.* **19,** 102–111 (1998).

Acknowledgements

The authors acknowledge funding from the EPSRC (EP/H000925/1) and the Leverhulme Trust (F/00025/Al). A.C. is a Royal Society Wolfson award holder. The authors thank J.T.A. Jones for assistance with NMR measurements.

Author contributions

A.C. conceived the project. T.M., D.A. and A.C. designed the experiments. T.M. prepared the cages and carried out the sorption experiments. K.J. conceived the modelling strategy and performed the molecular simulations. M.S. solved the single-crystal structures and S.C. refined the powder X-ray diffraction data. T.M. and A.A. performed the breakthrough experiments.

Additional information

Supplementary information and chemical compound information are available in the online version of the paper. Reprints and permission information is available online at http://www.nature.com/reprints. Correspondence and requests for materials should be addressed to A.I.C.

Competing financial interests

The authors declare no competing financial interests.

© 2013 Macmillan Publishers Limited. All rights reserved.